All-optical modulation of laser light in amorphous silicon–filled microstructured optical fibers. Appl. Phys. Lett. 91, 161112

ARTICLE *in* APPLIED PHYSICS LETTERS · OCTOBER 2007

Impact Factor: 3.3 · DOI: 10.1063/1.2790079

All-optical modulation of laser light in amorphous silicon-filled microstructured optical fibers

Dong-Jin Won, Mariola O. Ramirez, Hoonsoo Kang, and Venkatraman Gopalan[a)]
Materials Research Institute and Department of Materials Science and Engineering, Pennsylvania State University, University Park, Pennsylvania 16802, USA

Neil F. Baril, Jacob Calkins, and John V. Badding[b)]
Materials Research Institute and Department of Chemistry, Pennsylvania State University, University Park, Pennsylvania 16802, USA

Pier J. A. Sazio
Optoelectronics Research Centre, University of Southampton, Southampton SO17 1BJ, United Kingdom

(Received 8 August 2007; accepted 6 September 2007; published online 17 October 2007)

Amorphous silicon is deposited within optical fibers by a high pressure microfluidic deposition process and characterized via Raman spectroscopy. All-optical modulation of 1.55 μm light guided through the silicon core is demonstrated using the free carrier absorption generated by a 532 nm pump pulse. Modulation depths of up to 8.26 dB and modulation frequencies of up to 1.4 MHz are demonstrated. © *2007 American Institute of Physics*. [DOI: 10.1063/1.2790079]

All-optical data processing and routing allow conversions to the electronic domain to be avoided, which are two of the major bottlenecks limiting the performance of current networks. One of the two main technological approaches to the all-optical domain is the planar optical integrated circuit. This embodiment has seen a lot of progress of late, seeking to integrate as many photonic functions as possible typically onto silicon substrates,[1–3] thus attempting to emulate the very low cost and very high performance of the electronic integrated circuit. The alternate approach is to use the optical data transport medium, i.e., the glass fiber itself, for signal processing functions.[4] However, the processing functions that can be realized by this approach are limited considerably by the bulk optical properties of silica. We are pursuing an alternative paradigm that integrates the optoelectronic functionality of bulk semiconductors into the optical fiber itself, an important step towards all-fiber optoelectronics.[5,6] We have shown that crystalline silicon and germanium wires and tubes can be deposited into the microscale to nanoscale arrays of pores of microstructured optical fibers (MOFs) by a high pressure microfluidic technique. In this previous reported work, amorphous silicon was deposited at low temperatures and then crystallized by annealing at higher temperatures.[7] For some in-fiber applications, however, amorphous silicon may have more desirable properties or be more easily fabricated. For example, it is useful in photovoltaic applications and with appropriate hydrogen treatment, it can also be used for low loss optical waveguides ($\leqslant$0.5 dB/cm) that have the advantage of not exhibiting scattering from grain boundaries.[8] The amorphous silicon is deposited within the fiber with silane precursor partial pressures as high as 3.8 MPa; such precursor pressures are necessary to overcome mass transport constraints and are far higher than ordinarily used for deposition of silicon materials. It is thus important to characterize the material properties of the amorphous silicon deposited at high pressure such as the degree of short range and medium range orders via Raman spectroscopy, as reported here. We compare the properties of the silicon deposited at high pressure with those of amorphous silicon deposited under more conventional conditions. Finally, as a proof of concept, we show that 1550 nm laser light waveguided within the amorphous silicon wires can be modulated at 1.4 MHz using the free carrier plasma-dispersion effect.[2]

Amorphous silicon wires and tubes were fabricated inside 6 μm diameter pores using two different source precursors: (1) a 5% partial pressure of silane in helium for sample 1 (S1) and (2) a 5% partial pressure of silane in a mixture of 10% hydrogen and 85% helium for sample 2 (S2). Both precursors were at the same total pressure of 38 MPa. The MOFs were heated to 480–495 °C in a tube furnace to induce thermal decomposition of silane while the precursors were flowing through the pores. The central hole in the amorphous silicon from which deposition occurs closes down to form a solid wire [Fig. 1(a)] a few centimeters into the heated zone for both S1 and S2. The aspect ratio of the amorphous silicon structures is ~4000.

Micro-Raman spectra were obtained using a Renishaw Invia spectrometer in a backscattering geometry with 633 nm laser excitation focused onto the amorphous silicon through the transparent silica cladding. The transverse acoustic (TA), longitudinal acoustic (LA), longitudinal optical (LO), and transverse optical (TO) modes are all Raman ac-

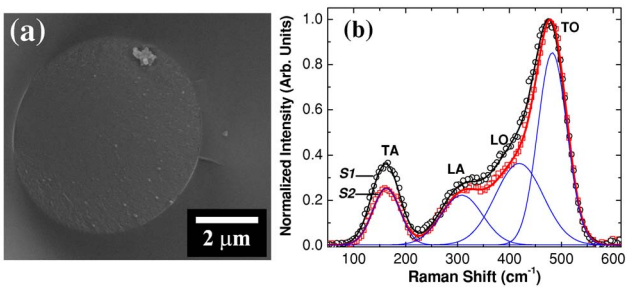

FIG. 1. (Color online) (a) Cross-sectional scanning electron micrograph of *a*-Si wire. (b) Micro-Raman spectra of *a*-Si wires inside MOFs. Solid lines are Gaussian fits to the TO, LO, LA, and TA phonon modes in *a*-Si.

[a)]Electronic mail: vxg8@psu.edu
[b)]Electronic mail: jbadding@chem.psu.edu

tive in amorphous silicon. The Raman spectra sample a broad range of the phonon density of states weighted by a coupling parameter.[9] The spectra for amorphous silicon are altered substantially by small changes in the degree of short range order (SRO) and medium range order (MRO). The peak position (ω_{TO}) and the full width at half maximum of the TO mode (Γ_{TO}) are associated with the force constant of the stretching vibration and the bond-angle deviation in tetrahedrally neighboring Si atoms.[10–13] Hence, the TO mode is known to probe the SRO. On the other hand, the TA mode, associated with bond bending, reflects dihedral angle variations, i.e., MRO.[12,13] A smaller ratio of the areas of the TA to TO modes (I_{TA}/I_{TO}) reflects a reduction in bond bending with respect to the stretching vibrations and is indicative of the improved MRO.[14,15] Normalized Raman spectra can be fit to four Gaussian functions corresponding to the four active Raman modes in amorphous silicon [Fig. 1(b)] for both samples. ω_{TO}, Γ_{TO}, and I_{TA}/I_{TO} are 482.2±1.5, 70.0±2.8, and 0.40±0.09, respectively, for the *a*-Si wire in S1 and 482.6±0.9, 66.2±2.6, and 0.30±0.08, respectively, for the *a*-Si wire in S2. A significant reduction in both the I_{TA}/I_{TO} ratio and Γ_{TO} is observed for S2 compared to S1, indicating that both the SRO and MRO are improved[14] by including hydrogen in the carrier fluid. The origin of this improvement remains uncertain; no Raman features in the region of 2000 cm^{-1} characteristic of Si–H or Si–H_x stretching modes are observed, although it is possible that some hydrogen below the limit of detection of Raman spectroscopy is incorporated. Increasing the partial pressure of hydrogen decreases the rate of decomposition of silane, which may allow for the improved SRO and MRO. The Γ_{TO} for S2 is comparable to the narrowest linewidths observed in device quality films as is ω_{TO}.[16]

Stress in semiconductor waveguides and devices can affect their properties. Upon chemically etching the silica cladding to reveal the amorphous silicon wires, a blueshift of ω_{TO} by about 1.1 cm^{-1} is observed, indicating that tensile stress resides in the wires due to the difference of thermal expansion coefficients between silica and the amorphous silicon. Similar behavior is observed in polycrystalline silicon-filled MOFs.[7]

The optical losses at 1.55 μm were measured to evaluate the performance of the amorphous silicon MOF waveguides. 8.0 and 9.6 mm long sections were cleaved from fully filled regions in S1 and S2. Laser light was coupled into a 6 μm diameter amorphous silicon core by a 40x objective lens and the light exiting the other side was then collimated by a 60x objective lens into an optical power meter. Index matching fluid was applied to strip cladding modes that can contribute to the output power. The propagation losses, including coupling losses, were estimated at 24.8 and 17.9 dB/cm in S1 and S2, respectively, by measuring the output at a fixed input power of 1 mW. In amorphous waveguides, propagation losses can originate from absorption by subgap states and scattering owing to the roughness at the core/cladding interface. Scattering losses at the core/cladding interface should be low because the silicon films are deposited on capillary walls with 0.1 nm rms roughness.[17] We note that achieving low scattering loss via fabrication of ultrasmooth waveguides remains a challenge in silicon photonics; even a few nanometers of roughness can result in significant loss because of the high index contrast between silicon and silica or air.[18] We attribute the improvement in loss for S2 by a factor of 5

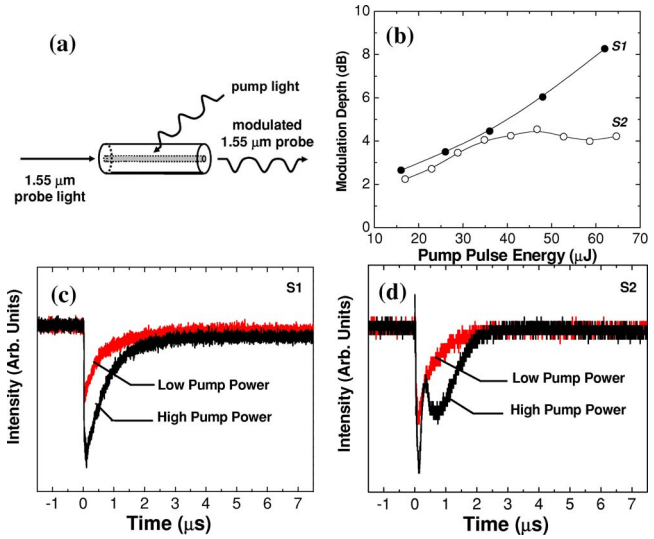

FIG. 2. (Color online) (a) Schematic diagram of all-optical modulation experiments with *a*-Si-filled MOF. (b) Modulation depth defined as $M(dB) = 10\log[1/[1-M(\%)]]$ vs pump pulse energy in S1 and S2 MOFs. $M(\%)$ is defined as the % change in the transmitted intensity upon modulation. Time resolved transmission of 1.55 μm probe signal under illumination from a 532 nm wavelength pump pulse recorded at two different energies: 16 μJ (low pump power) and 62 μJ (high pump power), for (c) S1, and (d) S2 fibers.

(~7 dB/cm) to a decrease in the defect density in the bandgap associated with the enhanced SRO and MRO. Further optimization of the high pressure deposition conditions should allow for further improvement in the intrinsic material absorption. The lowest loss amorphous silicon waveguides are hydrogenated to passivate dangling bonds and defects.[8] Deposition via thermal decomposition of silane alone typically does not lead to high quality hydrogenated materials with good optical and electrical properties because the temperatures required preclude significant incorporation of hydrogen.[19] Thus, plasma-enhanced deposition techniques that add additional energy to a low pressure precursor mixture are typically employed to synthesize high quality hydrogenated material. However, silicon particles homogeneously nucleated and grown in the gas phase with precursor pressures of 2 MPa can have hydrogen contents as high as 5 at. % as a result of the significantly altered reaction chemistry at high pressure.[20] Thus, it should also be possible to incorporate hydrogen into films heterogeneously nucleated and deposited at high pressure, such as those reported here, without the need for plasma enhancement, which is impractical in the capillary geometry.

The free carrier plasma-dispersion effect, the change of refractive index and absorption resulting from a change in the concentration of free carriers, can be used for silicon-based integrated modulators on planar platforms to achieve intensity or phase modulation.[1,21,22] A change in the carrier density can be induced either by carrier injection with a *p-n* junction or by photoexcitation with light. The all-optical, in-fiber modulator described here utilizes the latter approach, as schematically illustrated in Fig. 2(a). The probe, 1.55 μm cw light from a tunable laser, is amplified to 20 mW by an erbium doped fiber amplifier and then coupled into the multimode amorphous silicon waveguides embedded in the MOFs. The guided beam is collimated and subsequently coupled into a 50 μm core silica multimode fiber that is connected to a 12 GHz dc-coupled photoreceiver used for

detecting the intensity changes of the probe signal. A *Q*-switched Nd:yttrium aluminum garnet laser produces second harmonic generated 532 nm pulses of ~17.5 ns width at 10 Hz repetition rate to excite electrons and holes into the extended states of amorphous silicon. This pump beam is focused to 2.325 mm×75 μm by a cylindrical lens (f =300 mm) for efficient photogeneration of the excess carriers. The speed of operation, which depends on the photoexcited carrier lifetime, and the modulation depth can be determined from the output of the photoreceiver. Modulation depth values as high as 8.26 dB for S1 and 4.22 dB for S2 were achieved under visible illumination when the incident pump pulse was fixed at 65 μJ [Fig. 2(b)].

In the low power regime (10–40 μJ), M linearly increases with the incident pump power in both S1 and S2. Within this power range, both samples present a single exponential decay rate in their time-resolved transmission signal of the guided 1.55 μm intensity with an effective lifetime τ_{eff}=690 ns [Figs. 2(c) and 2(d)]. Thus, considering surface and Auger recombination as the dominant recombination processes,[21] this would lead to a free carrier density on the order of 10^{17}–10^{18} cm^{-3} (see Ref. 21), in excellent agreement with previous works where carrier densities of at least 5×10^{17} cm^{-3} were required for IR light modulation.[2,21,23,24] At higher input powers, a time gap between pump and the transmittance minima of ~80 ns (S1) and ~110 ns (S2) arising from ambipolar diffusion of excess carriers and field distribution of guided modes in amorphous silicon core was observed in both samples. Nevertheless, the most remarkable difference between both MOFs accounts from the appearance of a second component in the time-resolved transmission signal of S2 under high pump powers [Fig. 2(d)]. The origin of this component is not well understood at present, and several mechanisms such as two-photon energy transfer, Auger recombination, or radiative interfacial states between crystalline and amorphous phases due to Si nanocrystallites embedded in a Si matrix should be considered.[25,26] We exclude the possibility of modulation due to the thermo-optic effect because a temperature change is not expected to significantly change the absorption of 1.55 μm light, which is far from the absorption bandedge of Si.

In summary, we have described the fabrication of hybrid fiber structures combining MOFs with extreme aspect ratio amorphous silicon wires prepared by a microfluidic high pressure process. Micro-Raman spectroscopy and optical loss measurements were systematically employed to characterize both structural and optical performances of amorphous silicon-filled MOFs. All-optical modulation using telecom 1.55 μm probe and 532 nm pump pulses with modulation depths larger than 8.26 dB is demonstrated.

Two of the authors (J.V.B. and V.G.) acknowledge support from the National Science Foundation (Grant No. DMR-0502906), the Penn State Center for Nanoscale Science, funded by NSF under Grant No. DMR-0213623, and the Penn State-Lehigh Center for Optical Technologies. Another author (P.J.A.S.) acknowledges the Engineering and Physical Sciences Research Council for the support.

[1] A. S. Liu, R. Jones, L. Liao, D. Samara-Rubio, D. Rubin, O. Cohen, R. Nicolaescu, and M. Paniccia, Nature (London) **427**, 615 (2004).
[2] R. A. Soref and B. R. Bennett, IEEE J. Quantum Electron. **23**, 123 (1987).
[3] B. Jalali and S. Fathpour, J. Lightwave Technol. **24**, 4600 (2006).
[4] N. J. Doran and D. Wood, Opt. Lett. **13**, 56 (1988).
[5] P. J. A. Sazio, A. Amezcua-Correa, C. E. Finlayson, J. R. Hayes, T. J. Scheidemantel, N. F. Baril, B. R. Jackson, D. J. Won, F. Zhang, E. R. Margine, V. Gopalan, V. H. Crespi, and J. V. Badding, Science **311**, 1583 (2006).
[6] J. V. Badding, V. Copalan, and P. J. A. Sazio, Photonics Spectra **40**, 80 (2006).
[7] C. E. Finlayson, A. Amezcua-Correa, P. J. A. Sazio, N. F. Baril, and J. V. Badding, Appl. Phys. Lett. **90**, 132110 (2007).
[8] A. Harke, M. Krause, and J. Mueller, Electron. Lett. **41**, 1377 (2005).
[9] R. Shuker and R. W. Gammon, Phys. Rev. Lett. **25**, 222 (1970).
[10] N. Maley and J. S. Lannin, Phys. Rev. B **36**, 1146 (1987).
[11] D. Beeman, R. Tsu, and M. F. Thorpe, Phys. Rev. B **32**, 874 (1985).
[12] M. Marinov and N. Zotov, Phys. Rev. B **55**, 2938 (1997).
[13] R. L. C. Vink, G. T. Barkema, and W. F. van der Weg, Phys. Rev. B **63**, 115210 (2001).
[14] P. Danesh, B. Pantchev, K. Antonova, E. Liarokapis, B. Schmidt, D. Grambole, and J. Baran, J. Phys. D **37**, 249 (2004).
[15] G. Morell, R. S. Katiyar, S. Z. Weisz, H. Jia, J. Shinar, and I. Balberg, J. Appl. Phys. **78**, 5120 (1995).
[16] A. H. Mahan, in *Properties of Amorphous Silicon and its Alloys*, EMIS Datareviews Series, Vol. 19, edited by T. Searle (IEE, London/INSPEC, London, 1998), pp. 39–46.
[17] P. J. Roberts, F. Couny, H. Sabert, B. J. Mangan, D. P. Williams, L. Farr, M. W. Mason, A. Tomlinson, T. A. Birks, J. C. Knight, and P. S. J. Russell, Opt. Express **13**, 236 (2005).
[18] J. S. Foresi, M. R. Black, A. M. Agarwal, and L. C. Kimerling, Appl. Phys. Lett. **68**, 2052 (1996).
[19] C. J. Giunta, R. J. Mccurdy, J. D. Chapplesokol, and R. G. Gordon, J. Appl. Phys. **67**, 1062 (1990).
[20] J. O. Odden, P. K. Egeberg, and A. Kjekshus, Sol. Energy Mater. Sol. Cells **86**, 165 (2005).
[21] S. Stepanov and S. Ruschin, Appl. Phys. Lett. **83**, 5151 (2003).
[22] Q. F. Xu, B. Schmidt, S. Pradhan, and M. Lipson, Nature (London) **435**, 325 (2005).
[23] A. Cutolo, M. Iodice, P. Spirito, and L. Zeni, J. Lightwave Technol. **15**, 505 (1997).
[24] J. P. Lorenzo and R. A. Soref, Appl. Phys. Lett. **51**, 6 (1987).
[25] L. Pavesi, L. Dal Negro, C. Mazzoleni, G. Franzo, and F. Priolo, Nature (London) **408**, 440 (2000).
[26] M. Fujii, M. Yoshida, Y. Kanzawa, S. Hayashi, and K. Yamamoto, Appl. Phys. Lett. **71**, 1198 (1997).